

# Prophylactic Effects of NFκB Essential Modulator–Binding Domain Peptides on Bone Infection: An Experimental Study in a Rabbit Model

Wen-Jiao Wu<sup>1,\*</sup>, Chang-Liang Xia<sup>1,\*</sup>, Shuan-Ji Ou<sup>1</sup>, Yang Yang<sup>1</sup>, Xiao-Zhong Zhou<sup>1</sup>, Yun-Fei Ma<sup>2</sup>, Yi-Long Hou<sup>2</sup>, Fa-Zheng Wang<sup>3</sup>, Qing-Po Yang<sup>3</sup>, Yong Qi<sup>1,4</sup>, Chang-Peng Xu<sup>1,4</sup>

<sup>1</sup>Department of Orthopaedics, Guangdong Second Provincial General Hospital, Guangzhou, Guangdong, People's Republic of China; <sup>2</sup>Department of Orthopaedics and Traumatology, Nanfang Hospital, Southern Medical University, Guangzhou, Guangdong, People's Republic of China; <sup>3</sup>Department of Orthopaedics, First People's Hospital of Kashgar Prefecture, Kashgar, Xinjiang, People's Republic of China; <sup>4</sup>The Second School of Clinical Medicine, Southern Medical University, Guangzhou, Guangdong, People's Republic of China

\*These authors contributed equally to this work

Correspondence: Yong Qi; Chang-Peng Xu, Tel +86-20-8916-8085, Email gd2hqy@163.com; gd2hxcpx@163.com

**Introduction:** Osteomyelitis is characterized by intensive inflammatory bone disease and remains a clinical challenge in orthopedic surgery, despite the advances made in medical and surgical therapies. *Staphylococcus aureus* a major causative agent of osteomyelitis, causing the progressive inflammatory destruction of bone. Prophylaxis of osteomyelitis during orthopedic surgery is necessary. NFκB essential modulator–binding domain (NBD) peptides are cell-permeable peptide inhibitors of the IκB-kinase complex. The prophylactic effect of NBD peptides in relieving inflammation and inhibiting bone defects in osteomyelitis is still under investigation. Our purpose was to determine the preventive effect of NBD peptides in *S. aureus* infection–induced bone defects in osteomyelitis.

**Methods:** An *S. aureus* osteomyelitis rabbit model was used in this study. The rabbits were divided into four groups: NBD, cefazolin, control, and PBS. Clinical and laboratory indicators of erythrocyte-sedimentation rate, CRP, and TNFα levels were assessed to monitor systemic reactions. The efficacy of NBD peptides in *S. aureus*–induced osteomyelitis was evaluated by radiological, histological, and microbiological examinations, immunohistochemistry, immunofluorescence, and micro-CT scans.

**Results:** In general, NBD peptides effectively reduced clinical signs in rabbits when compared with the control group. Radiography indicated that there was more severe osteomyelitis in the bacterium-infection control group. There was no significance between cefazolin- and NBD-group average scores. The histological results of the lesion slices further confirmed different severity among the groups. Additionally, significant pathological differences were found between the cefazolin and NBD groups, and the PBS group showed no obvious pathological changes.

**Conclusion:** Prophylactic administration of NBD peptides to bone-defect areas inhibited bacterial spread and promoted bone regeneration, making NBD peptides a possible treatment option for prophylaxis in bone infections.

**Keywords:** NBD peptide, bone infection, *Staphylococcus aureus*, osteomyelitis

## Introduction

Osteomyelitis, which was named by Nelaton in 1844, is defined as an inflammation of bone tissue caused by an infectious agent, with most cases occurring after trauma to bone, bone surgery, or secondary to vascular insufficiency.<sup>1</sup> Osteomyelitis may be classified into acute and chronic forms.<sup>2</sup> Acute osteomyelitis involves progression from days to a few weeks and is based on acute symptoms, such as fever, leukocytosis, lymphadenopathy, and swelling to the affected area.<sup>3</sup> Cellulitis and trismus may also be present in the acute phase. Acute osteomyelitis may present as a routine infection and may take up to 10 days for bone loss to be radiographically apparent.<sup>2</sup> Patients may require hospital admission for intravenous antibiotics.<sup>2</sup> Chronic osteomyelitis is a relapsing and persistent infection spanning months to years with characteristic low-grade inflammation, presence of dead bone, new bone apposition, and fistulous tracts, with

treatment requiring (possibly multiple) surgical interventions and long-term broad-spectrum antibiotics.<sup>3</sup> Symptoms include swelling, pain, purulence, intraoral and extraoral draining fistulae, and nonhealing bony and overlying soft-tissue wounds.<sup>4</sup>

Antimicrobial therapy and surgical debridement are the primary modalities of osteomyelitis treatment, although often it is associated with a prolonged course, requiring a large commitment of patient and clinician as well as high health-care costs. The optimal type, route of administration, and duration of antibiotic treatment remain controversial, and the emergence of multidrug-resistant organisms poses major therapeutic challenges. Identification of the causative agent and subsequent targeted antibiotic treatment have a major impact on patient outcomes. Despite surgical and chemotherapeutic advancements, osteomyelitis remains difficult to treat, and no universally accepted protocol for treatment exists. Therefore, the development of various prophylactic measures for treating chronic osteomyelitis is increasingly important for future breakthroughs.

*Staphylococcus aureus* is a major pathogenic factor of human osteomyelitis.<sup>1</sup> Osteomyelitis is defined as an inflammation of bone tissue caused by an infectious agent.<sup>5</sup> Proinflammatory cytokines, such as IL1, IL6, and TNF $\alpha$ , are produced in *S. aureus*-induced osteomyelitis.<sup>5</sup> Overwhelming cytokine secretion breaks the balance between bone formation and resorption. TNF $\alpha$  has long been recognized as a key factor contributing to the pathogenesis of osteomyelitis and regulating bone mass. Osteoblast differentiation is crucial for ossification. TNF $\alpha$  promotes the differentiation of marrow-derived macrophages into osteoclast cells.<sup>6</sup> In addition, TNF $\alpha$  suppresses bone formation, and can inhibit the differentiation of osteoblasts.<sup>7</sup> Importantly, TNF $\alpha$  is a key player contributing to the pathogenesis of osteomyelitis,<sup>8</sup> against which TNF $\alpha$  inhibitors have been suggested as an alternative therapy.<sup>9</sup> IL1 and IL6 affect osteoblasts, and upregulated expression of IL1 or IL6 induces expression of the osteoclast-differentiation factor RANKL, leading to bone resorption.<sup>10</sup> Therefore, in addition to conventional antibiotic treatment, controlling defects and formation of bones is equally important.<sup>11</sup>

Major signal-transduction events triggered by RANKL and TNF $\alpha$  in various cell types lead to activation of the NF $\kappa$ B family.<sup>12</sup> NF $\kappa$ B is activated upon dissociation from the inhibitory protein I $\kappa$ Ba, an event following the phosphorylation of I $\kappa$ Ba by the upstream I $\kappa$ Ba-kinase (IKK) complex.<sup>13</sup> Studies have identified a specific region in the C-terminal of IKK $\alpha$  (L738–L743) and IKK $\beta$  (L737–L742) that is essential for adequate assembly of the IKK $\alpha/\beta$ -NF $\kappa$ B essential modulator (NEMO) complex, accordingly named the NEMO-binding domain (NBD).<sup>14,15</sup> Based on this region, several cell-permeable NBD peptides have been characterized, providing an opportunity to selectively abrogate proinflammatory NF $\kappa$ B activity in preclinical experimental models of inflammatory diseases.<sup>16–19</sup> Myriad publications are available reporting successful treatment of synovial inflammation,<sup>20</sup> inflammatory osteolysis,<sup>21</sup> inflammatory arthritis,<sup>22</sup> cartilage degradation,<sup>23</sup> and muscular dystrophy<sup>24</sup> by NBD peptides. Interestingly, studies have also shown the use of NBD peptides to attenuate IKK-complex assembly, inhibit NF $\kappa$ B activation, and prevent TNF $\alpha$ -induced osteoclastogenesis.<sup>22,25</sup> Our previous findings indicate that NF $\kappa$ B activation inhibits the osteoblast differentiation induced by TNF $\alpha$  and that the application of NBD peptides reduces this inhibitory effect.<sup>26</sup> However, further research is needed to confirm whether preventive use of NBD peptides can relieve inflammation and inhibit bone defects in osteomyelitis. The present study was conducted to investigate the prophylactic efficacy of local NBD-peptides therapy in the course of chronic osteomyelitis in a rabbit model.

## Methods

### Animals and NBD-Peptide Synthesis

The study was approved by the Institutional Animal Care and Use Committee prior to commencement. A total of 44 male healthy and pathogen-free adult New Zealand White rabbits (8–12 weeks old, 2.8–3.2 kg) were randomly assigned into four groups: NBD (12 rabbits), cefazolin (12 rabbits), control (12 rabbits), and PBS (eight rabbits). Cell-permeable NBD peptides (YGRKKRRQRRR-G-TTLDWSWLQME; Shanghai Apeptide) was synthesized and purified in accordance with our previous study.<sup>26</sup>

### Induced Rabbit Osteomyelitis Model

The rabbit chronic osteomyelitis model has previously been used to induce infection in tibiae with methicillin-sensitive *S. aureus* (American Type Culture Collection 25,923). Blood agar plates (Oxoid) were used to incubate the bacteria, and

five colonies of *S. aureus* were transferred and incubated at 37°C for 24 hours in trypticase soy broth (Oxoid). Subsequently, the bacterial cultures were washed twice and then aliquots of the organisms frozen at -80°C. After thawing the frozen aliquots before surgery, bacterial strains were grown in trypticase soy broth (TSB) overnight at 37°C with shaking at 225 rpm, subcultured at a dilution of 1:100, grown to mid-exponential phase, and centrifuged at 3000 rpm for 10 minutes. The pellets were washed and suspended with PBS to the desired concentration. A bacterial suspension in PBS was prepared, and a volume of 0.1 mL ( $10^6$  CFU) was injected into rabbit tibiae to induce osteomyelitis. The same inoculum was serially diluted and applied to blood agar after surgery and the number of bacteria confirmed by colony count after incubation at 37°C for 24 hours.

Following the protocol of Nijhof et al,<sup>27</sup> the rabbit osteomyelitis model was induced. Rabbit weights were recorded and anesthesia performed with pentobarbital sodium (3%) under strict aseptic conditions. The operation area of the proximal right tibia was shaved, disinfected with povidone-iodine, covered with sterile drapes, and then injected for local anesthesia with lidocaine (5 mg/kg). Usually, a 2 cm skin incision is made on the anterior lateral surface of the right proximal tibia and the cortex of the metaphysis partially exposed. A hole was drilled in the cortex using a 2mm Kirschner wire and subsequently irrigated with saline, and then bone marrow was extracted with an 18-gauge needle inserted into the medullary canal. Sequentially, 0.1 mL 5% sodium morrhuate, 0.1 mL bacterial suspension ( $10^6$  CFU/mL), and 0.1 mL saline (0.9%) were injected into the medullary cavity. The NBD group was treated with local percutaneous injection of a single dose of NBD peptides (5 mg/kg) into the medullary cavity (immediately after *S. aureus* inoculation), while the cefazolin group was treated with a cefazolin regimen (30 mg/kg) through the auricular vein beginning at 1 hour preoperatively. The control group received no further injections. The PBS group, operated on in parallel, was injected with equal volumes of 5% sodium morrhuate in PBS instead of the bacterial suspension. The surgery hole was sealed with sterile bone wax to prevent injection leakage, the area rinsed, and the fascia, subcutaneous layer, and skin sewn up with 4/0 Vicryl Ethicon (Somerville). Postoperative follow-up lasted 28 days, during which time the animals were housed in separate cages and fed a normal diet.

## Clinical and Laboratory Monitoring

The temperature and body weight of the rabbits were recorded daily. After the initial operation, all animals were followed closely to detect clinical signs of septic spread. Blood samples were collected for leukocyte counts, erythrocyte-sedimentation, rate and CRP- and TNF $\alpha$ -level measurements preoperatively and on days 3, 7, 14, 21, and 28 postoperatively.

## Radiological Analysis

On days 1, 7, 21, and 28 postoperatively, standard anteroposterior and lateral radiographs were taken. According to the severity-score system for osteomyelitis described by Norden et al,<sup>28</sup> the radiographs were randomized and scored by an orthopedic surgeon in a blinded fashion. A composite score was obtained after the total tibial length was taken into account, and the animals were diagnosed with osteomyelitis when the score was  $\geq 3$ .

## Microbiological Analysis

On day 28 postoperatively, blood samples were extracted and the rabbits killed by intravenous injection of pentobarbital sodium. Tibiae were excised and freed from soft tissue under aseptic conditions. They were all cut into three parts — the proximal metaphysis (section A), diaphysis (section B), and distal metaphysis (section C) — using a swing saw under continuous normal saline irrigation. A 1 cm part of the proximal area of section B (section B1) was for microbiological analysis, and 1 cm parts of the middle of section B (section B2) and remaining parts (sections A and C) were for histological examination (Figure 1A).

A portion of bone was cut from section B1 for microbiological analysis. Using a tissue homogenizer (BioVision), the bone sample was homogenized in 30 mL sterile PBS at 10,000 rpm for 5 minutes. After tenfold dilution prepared in saline, a series of each 10  $\mu$ L dilution was seeded on a blood agar plate and incubated for 48 hours at 37°C. Finally, bacterium colonies from the bone tissue were counted. For detection-limit values for statistical analysis, negative cultures were calculated conservatively as  $2 \times 10^3$  CFU/g, and all tests were carried out in triplicate under aseptic conditions.

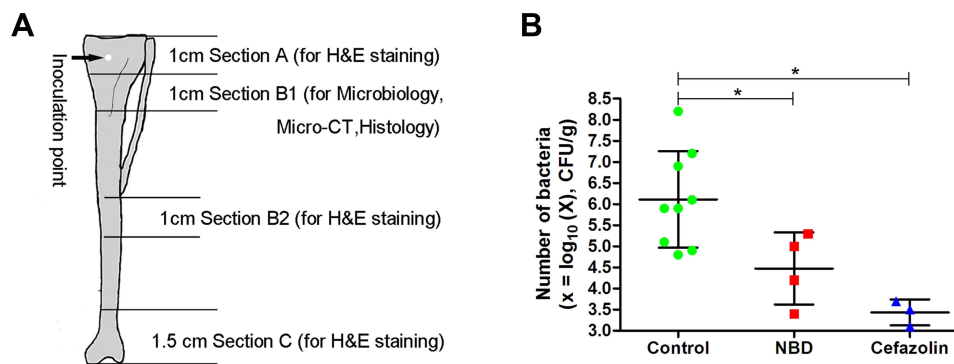


**Figure 1** (A) Tibiae were cut into A, B, and C sections. A 1 cm part of the proximal area of section B (section B1) was for microbiological analysis, and a 1 cm part of the middle of section B (section B2) and all remaining parts (sections A and C) were for histological examination. All tibia parts were used for H&E staining to confirm the severity of osteomyelitis, except section B1, which was used instead for microbiological analysis, micro-CT measurement, and histological examination with Masson staining, immunohistochemistry, and immunofluorescence. (B) Bacterial numbers in bone tissue in the control group (n=9), NBD group (n=4), and cefazolin group (n=3). Student's t-tests were conducted to compare the control and NBD/cefazolin groups. \* $p < 0.05$ .

## Histological and Immunohistochemical Analysis

H&E staining were conducted for bone samples. Decalcified cross-sections (5  $\mu\text{m}$ ) were assessed by a pathologist in a blinded fashion in accordance with the scoring system devised by Smeltzer et al.<sup>29</sup> Animals were diagnosed as having osteomyelitis when their samples scored 4 points or more. To detect existing systemic side effects of the NBD peptides, cross-sections of hearts, livers, spleens, lungs, and kidneys of the animals in the NBD group were also examined macroscopically and histologically to identify bacterial spread, abscess formation, and/or any signs of septic reaction.

Immunohistochemistry of osteocalcin (Ocn) and Runx2 was performed using antibodies of Ocn (ab93876, Abcam) and Runx2 (ab192256, Abcam) at 1:100 dilution. Specimen sections were washed with PBS and blocked with 5% serum for 30 minutes. Then, each sample was stained with primary antibodies at 4°C. Subsequently, the samples were rinsed with PBS and incubated with goat antirabbit secondary antibodies at 37°C for 30 minutes. After treatment with 3,3'-diaminobenzidine tetrahydrochloride solution, the sections were counterstained with hematoxylin to produce a brown precipitate at the antigenic site. Slides were observed and images captured by a microscope. All animals were assessed in our experiment. For the sample of each animal, four fields of each section were randomly selected and positive-expression rate and gray values of stained areas measured under the same light intensity to semiquantify protein-expression levels using Image Pro Plus 6.0 (Media Cybernetics).

## Masson Staining

Masson trichrome staining was used for the detection of collagen fibers in tissue. Tissue sections were deparaffinized in xylene and rehydrated in a graded alcohol series, then were mordant in Bouin's solution at 37°C for 2 hours. Bouin's solution was made with 75 mL saturated picric acid, 25 mL 10% formalin solution, and 5 mL acetic acid. Sections were stained using a Masson's trichrome staining kit (Phygene) following the manufacturer's instructions. Areas of the collagen-fiber layer stained blue were calculated using Image Pro Plus 6.0.1.

## Immunofluorescence

Immunofluorescence staining for CD31 and  $\alpha$  smooth-muscle antibodies (SMAs) was done according to the standard protocol. Pretreated paraffin slides were blocked in 5% serum prior to the addition of primary antibodies: rabbit anti-CD31 (1:100, Abbiotec) and mouse anti- $\alpha$ SMAs (1:50, Abcam). Incubation with the secondary antibodies rhodamine-conjugated goat antirabbit (1:50, Abcam) and FITC-conjugated goat antimouse (1:50, Dako) was carried out for 30 minutes. Then, samples were stained with DAPI, fixed in 5% paraformaldehyde, and stored until image acquisition by CLSM. The quantity of mature blood vessels was assessed in sections stained with positive CD31 and SMAs per area. We took four fields for every sample, all animals were included for analysis, and the data in this manuscript are representative of each experimental group.

## Micro-CT Measurement

For tibiae harvested at 4 weeks postoperatively, samples were first analyzed by micro-CT prior to the histological preparations. Morphology of the reconstructed tibial cortex was assessed using an animal micro-CT scanner (Explore Locus, GE Healthcare). After micro-CT scans, defect regions were identified by contours as traced regions of interest, the relative measurements of which were calculated, including bone-mineral density (BMD) and bone volume/total volume (BV/TV). Quantitative analysis of the newly formed bone was performed using morphometrical methods. Three-dimensional isosurface renderings were done for visualization of bone. To obtain parameters of BV fraction and BMD in defect areas, gray values of the pixels were stratified in a histogram running from 225 to 500 with a range of 25. Micro-CT measurements included BV/TV and local BMD in the bone defect.

## Statistical Analysis

SPSS 11.0 for Windows was used to analyze the results. Mann–Whitney tests for independent samples were performed to compare laboratory values and radiological and histological scores across the groups. Newly formed BV was compared with ANOVA. Unless stated otherwise, results are presented as means  $\pm$  standard deviation, and  $p \leq 0.05$  was considered significant.

## Results

### General Conditions

Clinical signs following initiation of infection varied from mild to severe. Two animals in the control group and one in the NBD group had to be killed before the 4-week end point. Two had bacterial empyema of the knee joint and the other showed progressive necrosis of the proximal tibia, probably due to prior sodium morrhuate injection. The remaining 41 animals were included in clinical signs data. In general, there was an acute phase within 7 days after rabbits had been infected with *S. aureus*. Temperature, leukocyte count, erythrocyte-sedimentation rate, CRP, and TNF $\alpha$  increased within 1 week, and showed a peak on day 7 postinoculation. There were significant differences detected in the NBD and cefazolin groups when compared with the control group on days 7 and 14, respectively, then there were fluctuations during follow-up with no obvious differences between the control group and the treatment groups (Figures 2 and 3). The weight of the rabbits in the control group decreased more quickly than the cefazolin group until day 14, then the weights in both groups recovered. In the NBD group, weights had decreased at 7 days postinfection, then increased gradually, representing earlier recovery state than the control group (Figure 2B).

### Treatment with NBD Peptides Reduced *S. aureus* Growth in Bone Tissue

On microbiological examination, methicillin-sensitive *S. aureus* was recovered from four of eleven, three of twelve, and nine of ten bone specimens from the NBD, cefazolin, and control groups, respectively. No bacteria number in the PBS group was detected. As Table 1 shows, quantitative data on bacterial culture numbers showed significantly fewer viable bacteria in the NBD ( $p=0.045$ ) and cefazolin ( $p=0.012$ ) groups than the control group. No significant difference was found between the NBD and cefazolin groups ( $p=0.154$ ; Table 1, Figure 1B). The bacterial strains cultured from samples

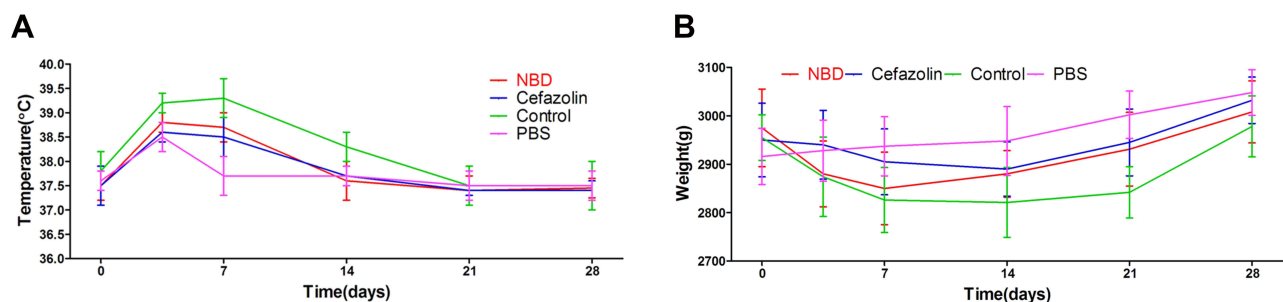


**Figure 2** Mean (A) body-temperature and (B) weight changes in the control group (n=10), NBD group (n=11), cefazolin group (n=12), and PBS group (n=8). No significant differences were observed before and on the 28th day after the operation, and there was no difference in body-temperature or weight changes within and between the groups.

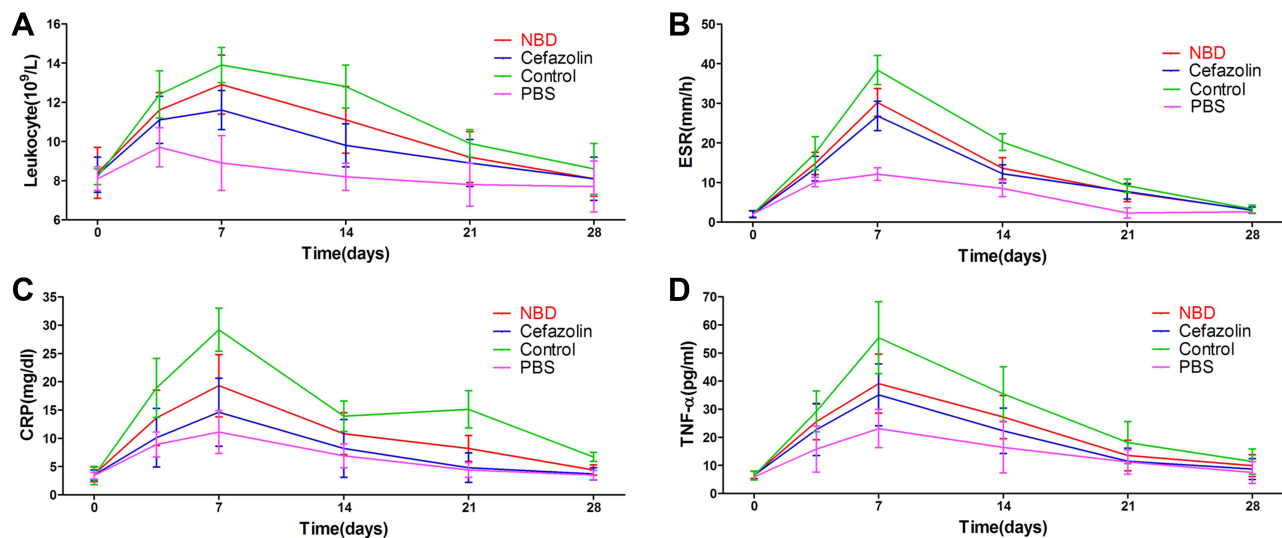


**Figure 3** Changes in (A) leukocyte count, (B) ESR, and (C) CRP, and (D) TNF $\alpha$  in the control group (n=10), NBD group (n=11), cefazolin group (n=12), and PBS group (n=8).

with positive culture results at autopsy were confirmed to be identical to those used for the induction of osteomyelitis. Therefore, no contamination of other bacterial strains was observed.

## NBD Peptides Relieved Osteomyelitis

Radiographs showed more severe osteomyelitis in the control group, with nine of ten animals having a score of 3 or above. Five of eleven and three of twelve animals in the NBD and cefazolin groups, respectively, had a score of 3 or above at autopsy, while no infection was observed in the PBS group (Figure 4). The total scores of the control group were significantly higher than those in the NBD group ( $p=0.008$ ) and the cefazolin group ( $p=0.001$ ). There was no statistically significant difference between the NBD and cefazolin groups ( $p=0.373$ ; Table 1).

## NBD Peptides Inhibited *S. aureus* Infection–Induced Inflammation in Bone Tissue and Accelerated New Bone Formation

Histological results further confirmed the varying severity of osteomyelitis among the groups (Figure 5). Typical signs of osteomyelitis, including intraosseous acute inflammation, intraosseous chronic inflammation, periosteal inflammation, and bone necrosis, were seen in some animals, while partial signs were noted in others. Based on the scoring system, a severity score of 4 or more was found in six of eleven, four of twelve, and nine of ten animals in the NBD, cefazolin, and control groups, respectively. The control group showed significantly higher scores than the NBD ( $p=0.002$ ) and cefazolin groups ( $p=0.001$ ). A statistically significant difference was also found between the NBD and cefazolin groups ( $p=0.035$ ; Table 1). No pathological changes were observed in the PBS group (Figure 5F). These findings

**Table 1** Radiological and histological scores and culture results of tibia specimens on autopsy

| Group            | Radiological            | Histological            | Bacterial culture           |  |
|------------------|-------------------------|-------------------------|-----------------------------|--|
|                  |                         |                         | Infection rate              | Bacterial Quantity (log <sub>10</sub> CFU/g) |
| NBD (n=11)       | 2.55±1.21* <sup>#</sup> | 6.09±3.11* <sup>▲</sup> | 4/11 (36.36%)* <sup>§</sup> | 4.47±0.85* <sup>◆</sup>                      |
| Cefazolin (n=12) | 2.08±0.67*              | 3.33±2.15*              | 3/12 (25%)*                 | 3.43±0.29*                                   |
| Control (n=10)   | 4.50±1.58               | 9.70±2.45               | 9/10 (90%)                  | 6.11±1.14                                    |
| PBS (n=8)        | 1.63±0.52               | 2.13±0.99               | NT                          | NT   |

**Notes:** Data presented as means ± SD. \* $p<0.05$  vs control group; <sup>#</sup> $p>0.05$  vs cefazolin group; <sup>▲</sup> $p<0.05$  vs cefazolin group; <sup>§</sup> $p>0.05$  vs cefazolin group; <sup>◆</sup> $p>0.05$  vs cefazolin group.

**Abbreviation:** NT, not tested.

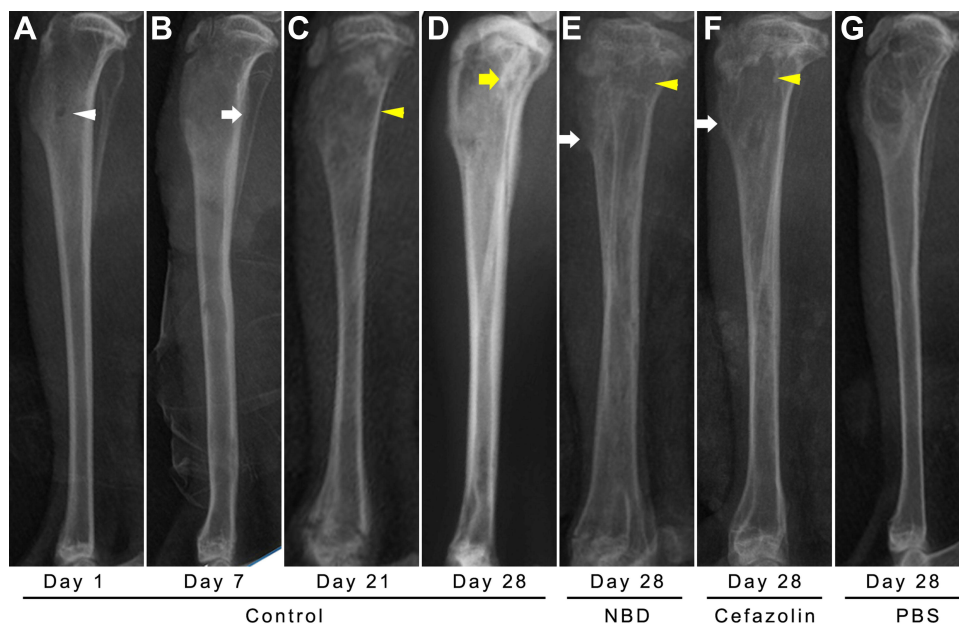


**Figure 4 (A–D)** In the control group (n=10), lateral tibial slices were taken on days 1, 7, 21, and 28, and lateral radiographs of tibiae showed the typical course, including drilling (white arrowhead), gradually aggravating the periosteal reaction and eventually forming new bones (white arrow), bone destruction (yellow arrowhead), and sequestra (yellow arrow). The lateral radiographs of the (E) NBD (n=11) and (F) cefazolin group (n=12) taken at the same time showed only mild–moderate periosteal reactions on day 28. (G) Lateral radiographs of the PBS group (n=8) showed no signs of osteomyelitis on the 28th postoperative day. All samples of animals were examined.

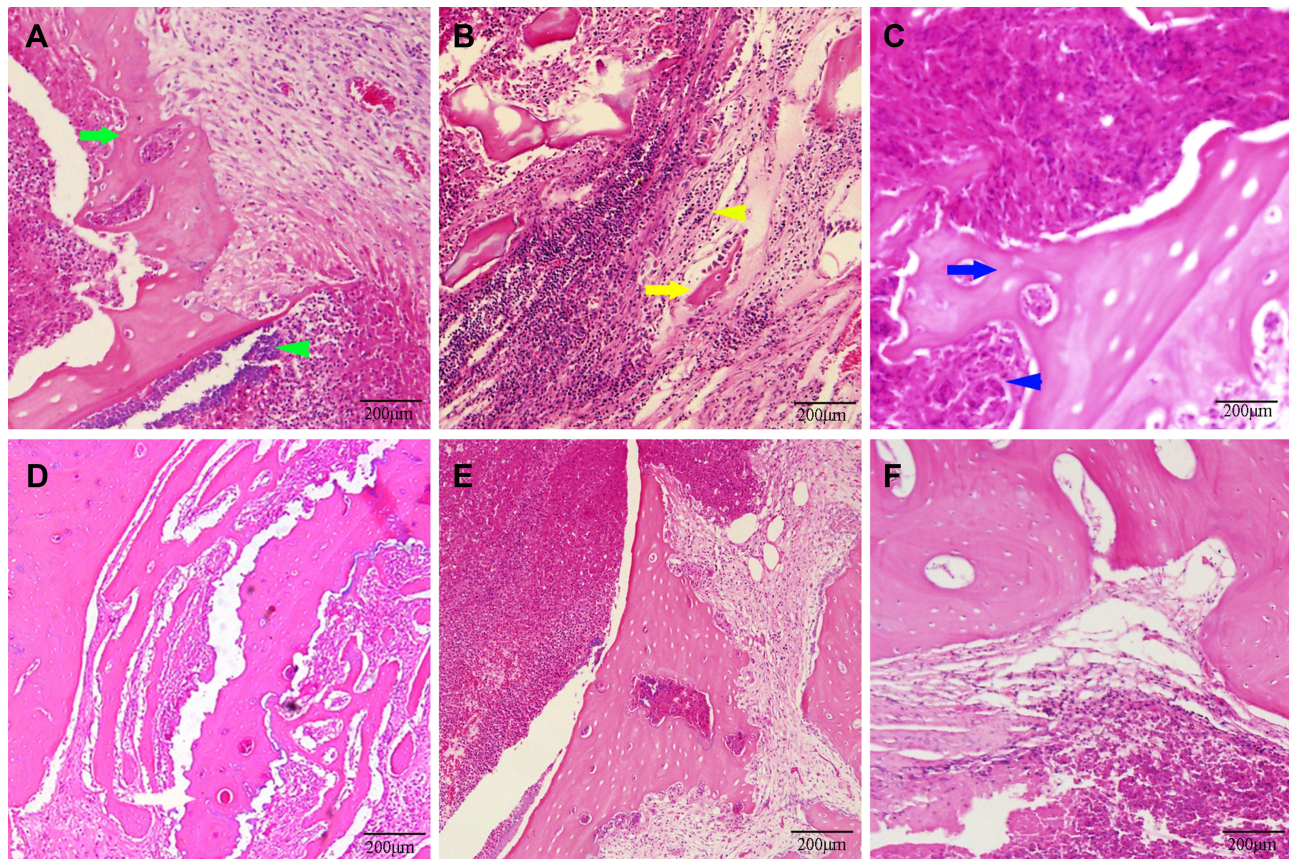


**Figure 5** Photomicrographs of the longitudinal section of the tibia in the control group (n=10) (A–C) showing cortical bone destruction, sequestrum formation (green arrow), severe inflammation with intramedullary abscess (green arrowhead), remodeled bone (yellow arrow), fibrosis (yellow arrowhead), periosteal new bone formation (blue arrow), and sequestrum surrounded by proliferated foamy histiocytes (blue arrowhead) with H&E. The NBD group (n=11) (D) and cefazolin group (n=12) (E) showed mild calcification and destruction of cortical bone, and new bone was found in the medulla, and in the PBS group (n=8) (F), there were **prompt normal bone**(H&E), respectively. All samples of animals were examined.

demonstrated that NBD and cefazolin may support in situ bone-infection control by effectively inhibiting inflammation. Bacterial growth was not originally detected in each blood culture taken before and 30 minutes after NBD-peptide application. Subsequently, H&E staining of hearts, livers, spleen, lungs, and kidneys of the animals also ruled out bacterial inoculation or abscess formation in these representative organs (Figure 6). Therefore, no bacterial spread of NBD peptides or any other systemic side effects were detected.

From the H&E results, new bone formation was observed in all groups, but critically differed among them. Masson staining was also chosen to evaluate osteogenic performance. Only a marginal amount of fibrous tissue filling the defects was formed in the control group (Figure 7A), whereas significantly enhanced bone formation occurred in the NBD and cefazolin groups, and the defects were filled mostly with newly formed bone tissue. Both mature (dark blue) and immature (light blue) bone tissue were observed (Figure 7B and C). New bone tissue almost completely covered defects in the cefazolin group, and bone tissue in the bone defects was primarily composed of mature bone tissue, stained a dark blue. In addition, quantitative analysis of new bone areas indicated that the NBD and cefazolin groups exhibited improved osteogenesis ability compared with the control group ( $p=0.03$  and  $p=0.01$ , respectively). No significant difference was found between the NBD and cefazolin groups in measurement of bone regeneration at the defect site ( $p=0.388$ ), demonstrating excellent activity of bone formation among them, although the cefazolin group exhibited the highest new bone area (Figure 7D).

### NBD Peptides Increased Osteogenic Marker Expression in Defect Areas

Expression of Ocn and Runx2,<sup>30,31</sup> two indicators of osteoblast differentiation, were examined to further confirm alterations in bone formation in defect areas. The results demonstrated that the NBD and cefazolin groups exhibited higher osteogenic marker expression for Runx2 and Ocn (brown staining) than the control group (Figure 8A–F). Further quantitative data determined by number of Ocn- and Runx2-positive areas (indicated by brown staining) on the level of Ocn expression in the NBD and cefazolin groups was significantly increased compared with the control group. However, no significant difference was found between the NBD and cefazolin groups in expression levels of Ocn ( $p=0.073$ ) or Runx2 ( $p=0.090$ ) at 4 weeks postoperatively in the defect area, and the NBD peptides improved osteogenic ability comparably to cefazolin (Figure 8G–H).

### Treatment with NBD Peptides Promoted Vascularization in Operation Area

Vascularization is a critical step in bone formation in newly formed tissue. Immunofluorescence-staining analysis for the vascular markers CD31 and  $\alpha$ SMA was conducted at 4 weeks to evaluate vascularization in the regenerated bone tissue (Figure 9A–C). The NBD and cefazolin groups had more circular blood vessels than the control group, indicating that more mature vessel tissue had been generated. Quantitative analysis of newly formed vessels and total vessels (Figure 9C and D) also revealed that their density and number had been significantly increased by NBD or cefazolin treatment compared with control group, whereas there was no significant difference between the NBD and cefazolin groups (Figure 9D) with regard to newly formed vessels density ( $p=0.288$ ). The number of new blood vessels increased significantly after treatment in the cefazolin group compared to the NBD groups ( $p=0.015$ , Figure 9E). These results demonstrate that the NBD intervention had almost the vascularization capacity of cefazolin in promoting bone formation.

### Micro-CT Revealed NBD Treatment Exhibited Greater New Bone Formation

Morphology of newly formed bone tissue was detected by micro-CT, and the results demonstrated that there was only scattered bone tissue close to the defect edges in the control group (Figure 10A), while defect areas showed obvious new bone formation in the NBD and cefazolin groups, although there were several cavities scattered over the area in the NBD groups (Figure 10B and C). Compared to the control group, the NBD group exhibited greater new bone formation, although the cortex was incomplete and there were voids beneath the cortex. In all groups, sporadic trabecular bone was observed in the marrow canal. Morphometric analysis was also used to calculate the amount of newly formed bone in the defect sites (Figure 10D and E). Although new BV calculation indicated that the cefazolin group had the best bone regeneration among the groups, there was no significant difference between

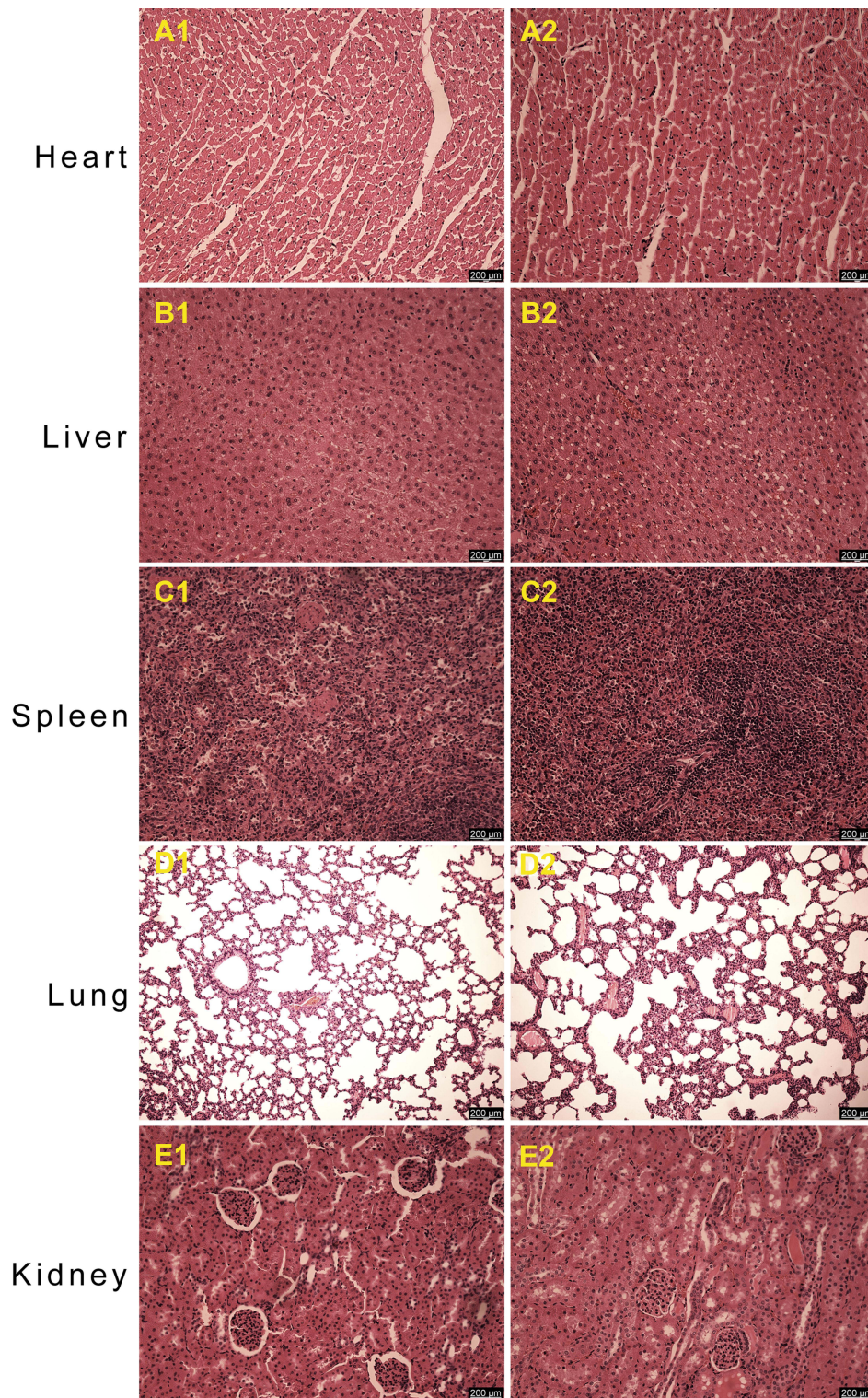


**Figure 6** On postoperative day 28, histological analysis of the heart (**A1** and **2**), liver (**B1** and **2**), spleen (**C1** and **2**), lung (**D1** and **2**), and kidney (**E1** and **2**) found no abnormalities. The upper row (**A1–E1**) is the control group (n=10), and the lower row (**A2–E2**) is the NBD group (n=11, H&E). All samples of animals were examined.

the NBD and cefazolin groups in BMD or BV/TV at the defect site ( $p=0.215$  and  $p=0.622$ , respectively). Meanwhile, the NBD group exhibited high levels of both BMD and BV/TV at the defect site when compared to control groups (both  $p=0.001$ ).

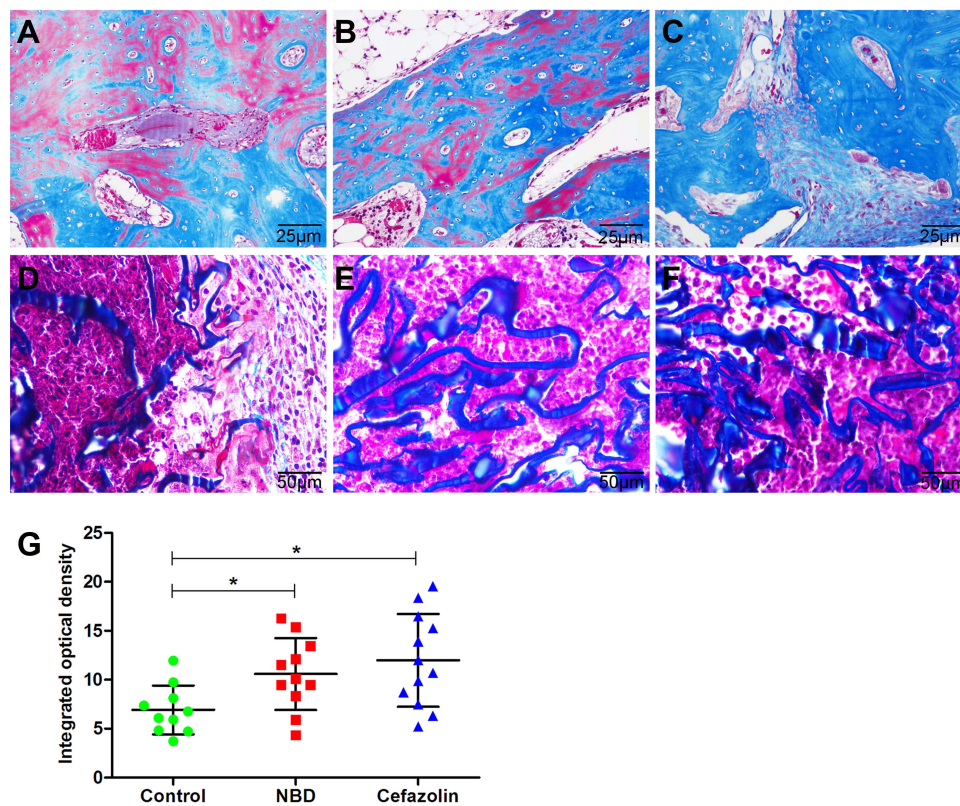


**Figure 7** Assessment of new bone tibia defects using Masson staining in the control (n=10) (**A** and **D**), NBD (n=11) (**B** and **E**), and cefazolin (n=12) (**C** and **F**) group at 4 weeks postoperatively. Quantitative analysis demonstrated improved osteogenic activity, and most defect areas in the NBD and cefazolin groups were filled with newly formed bone tissue (**D**). \* $p < 0.05$  (**G**).  $p$ All samples of animals were examined.

## Discussion

Osteomyelitis is an acute or chronic infection of the bone characterized by suppurative inflammation, abnormal bone remodeling, and uncontrolled bone defects.<sup>34</sup> Antibiotic selection is still considered a difficult cure for osteomyelitis, although the risks of adverse reactions due to prolonged and widespread use of antibiotics have been discussed. *S. aureus* is the most common cause of bone infection.<sup>32,33</sup> For bone infected with *S. aureus*, recent studies have emphasized the importance of NF $\kappa$ B in the host's early innate immunoresponse. NF $\kappa$ B activation includes the canonical and noncanonical NF $\kappa$ B-signaling pathway. The latter selectively activates p100-isolated NF $\kappa$ B members, mainly NF $\kappa$ B2 p52 and RelB, and plays a role in innate and adaptive immunoresponses.<sup>15</sup> NBD peptides selectively abrogated the inflammation-induced activation of NF $\kappa$ B by targeting the NBD–NEMO interaction. Rationales for treating chronic inflammatory diseases involving bone resorption with NBD peptides have been documented, reducing levels of TNF $\alpha$  and destruction of bone based on NF $\kappa$ B blockade.<sup>25</sup> Downstream NF $\kappa$ B proinflammatory cytokines, such as TNF $\alpha$  and IL6, produced in *S. aureus*–induced osteomyelitis cause progressive inflammatory destruction of bone.

Drugs that selectively target inflammation rather than bacterial infection itself would be of better therapeutic value and would likely display fewer undesired side effects and drug resistance. NF $\kappa$ B regulates the inflammatory response leading to the development of bone infection, and selective blocking of NF $\kappa$ B could have prophylactic implications in preventing the disease. NBD peptides have been reported to modulate inflammation and osteoclastogenesis.<sup>29,34</sup> Based on our previous study, NBD peptides also promoted osteoblast differentiation impaired by TNF $\alpha$ . A possible underlying mechanism is that NBD peptides selectively attenuate the activation of NF $\kappa$ B by targeting NEMO and further abrogate (at least partly) the inhibitory effect of inflammation on osteoblast differentiation.<sup>14,15</sup>

NBD peptides exhibited efficacy in infection prevention, with lower infection rate, bacterial quantity, and radiological and histological osteomyelitis scores comparable to cefazolin, providing an opportunity to selectively abrogate the

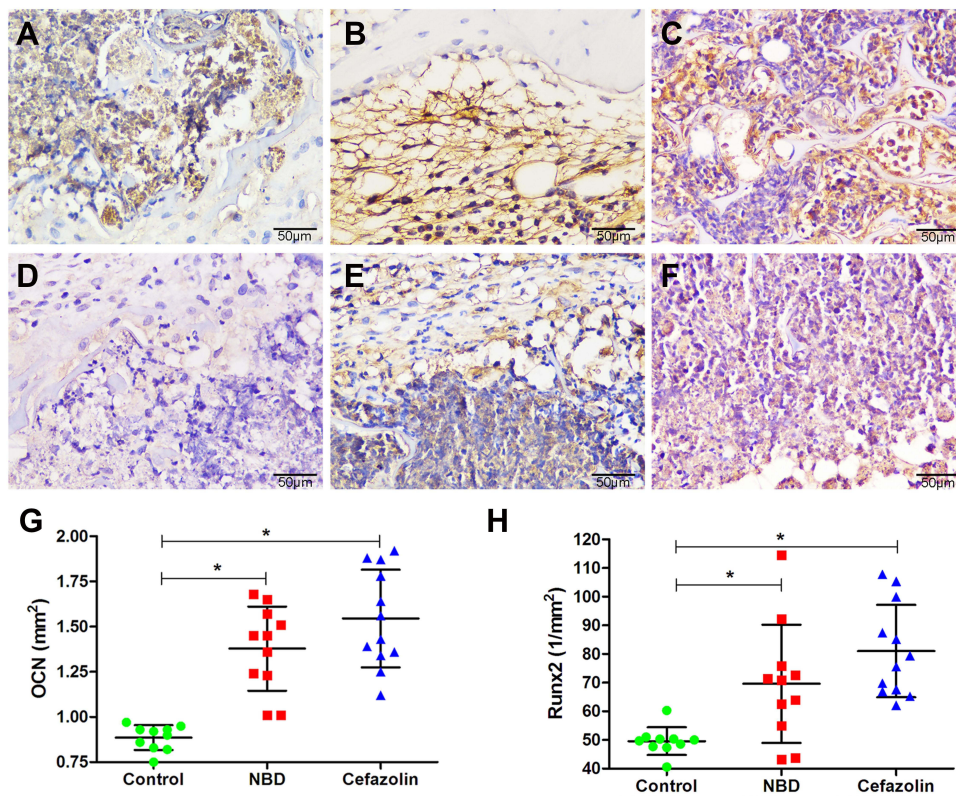


**Figure 8** Immunohistochemical staining of Ocn and Runx2 of tibia defects at 4 weeks postoperation. Ocn expression in tissue sections of defect areas in control (A), NBD (B), and cefazolin (C) groups, and Runx2 expression in tissue sections of defect areas in control (n=10) (D), NBD (n=11) (E), and cefazolin (n=12) (F) groups. Quantitative analysis demonstrated strong positive staining of Ocn (G) and Runx2 (H) of the defect areas in the NBD and cefazolin groups, in contrast to the control group. \**p*<0.05. Ocn, osteocalcin. All samples of animals were examined.

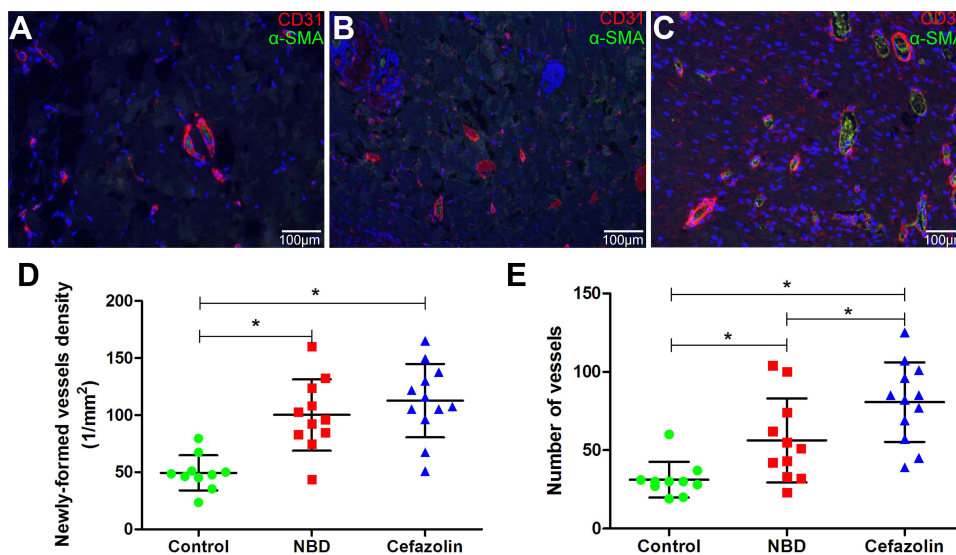


**Figure 9** Fluorescence staining of tibial defect sections. Confocal laser-scanning images of αSMA and CD31 staining for bone defects in control (n=10) (A), NBD (n=11) (B), and cefazolin (n=12) (C) groups after 4 weeks. With DAPI, nucleus are counterstained blue. At 4 weeks after intervention, data of neovascularization and physiologically appropriate blood-vessel circumference were normalized to the tissue area (the number of blood vessels/mm<sup>2</sup>) (D and E). \**p*<0.05. All samples of animals were examined.

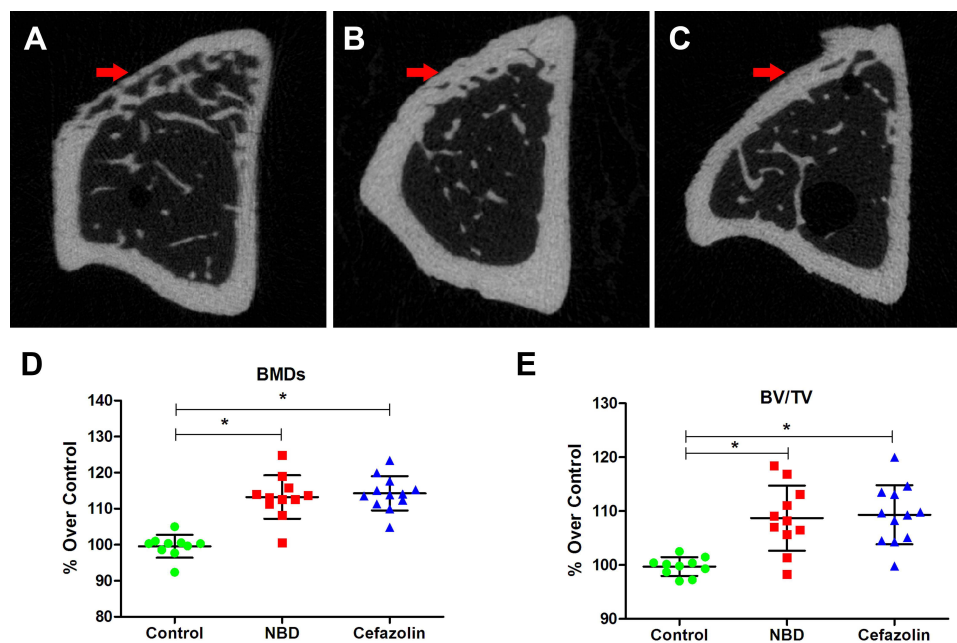


**Figure 10** Four weeks after operation, microscopic CT cross-sectional analysis of the proximal tibia bone defect in the control (n=10) (A), NBD (n=11) (B), and cefazolin (n=12) (C) groups. Morphological measurement of bone-mineral density (BMD) (D) and bone volume/total volume (BV/TV) (E) was used to evaluate the local defect area. Variance-test results were used to assess the data. \* $p < 0.05$ . All samples of animals were examined.

*S. aureus*-induced activation of NF $\kappa$ B. Due to its good anti-inflammatory and osteogenic ability in vitro, a rabbit model with bone infection was selected to confirm the effect of NBD peptides on bone regeneration. The results of histological analysis were consistent with the conclusions drawn by micro-CT in our study. Detection of the osteogenic markers Runx2 and Ocn showed that NBD peptides can effectively promote osteoblast differentiation in vivo, thereby promoting bone growth. Correspondingly, vascularized bone regeneration also occurred after NBD-peptide intervention, perhaps owing to selective abrogation of the inflammation-induced activation of NF $\kappa$ B. Local NBD-peptide therapy in vivo exhibited a possible strategy to prevent bone infection. NBD peptides have the potential to ameliorate the progression of bone infection and promote osteogenesis.

Extensive chronic osteomyelitis was achieved within 3 weeks of *S. aureus* infection based on the well-established animal models.<sup>27,35</sup> *S. aureus* is the major pathogen among staphylococci, the most common cause of bone infection, and also activates the NF $\kappa$ B pathway.<sup>32,33</sup> Our in vivo study of *S. aureus* infection showed that NBD peptides exhibited infection-prevention efficacy, with lower infection rate and bacterial quantity, as well as radiological and histological scores for osteomyelitis, comparable to cefazolin, providing an opportunity to selectively abrogate the *S. aureus*-induced activation of NF $\kappa$ B. Various prophylactic measures, including perioperative antibiotic prophylaxis, have been used with varying success to reduce the incidence of bone infection in orthopedic surgery.<sup>36</sup> In the clinic, one antibiotic treatment is usually used as prophylaxis to prevent infection during surgery. We used cefazolin to treat rabbits once before surgery as a positive control. To observe drug toxicity, clinical signs, laboratory monitoring, blood culture, and histological examination of hearts, livers, spleens, lungs, and kidneys was performed after treatment with NBD polypeptides. A high bacterial count was considered to indicate a high risk of bacterial spread. Whether clinical or laboratory signs showed bacterial spread, bacterial growth in blood cultures after NBD-peptide intervention was not observed, and there were no secondary infections in organs on histological examination. However, despite acute active bacterial infection in animals representing a worst-case scenario of chronic bone infection,<sup>37</sup> after NBD-peptide intervention, good results were obtained and no spread of infection was detected. Interestingly, NF $\kappa$ B has an important antiapoptotic effect under physiological conditions, but in a drug its application may cause extensive apoptosis.<sup>25</sup> Studies have confirmed this view,<sup>21,22</sup> but treatment of chronic inflammatory diseases by blocking NF $\kappa$ B rarely has side effects. Local administration also further reduces the potential toxicity of the drug. Through local injection of NBD polypeptides, we did not find any side effects or bacterial spread in the rabbit model, thus confirming this view.

As indicated in previous research, macrophages must activate NFκB for phagocytosis of *S. aureus*.<sup>33</sup> For bone infection with *S. aureus*, recent studies have also emphasized the important role of NFκB in early innate immunoresponse. NFκB activation involves the classic NFκB-signaling pathway and the noncanonical NFκB-signaling pathway. The non-canonical NFκB-signaling pathway selectively activates p100-isolated NFκB members, mainly NFκB2 p52 and RELB. Recently, studies have shown that the nonstandard NFκB pathway plays a role in innate and adaptive immunoresponses.<sup>15</sup> We speculated that the cell-permeable NBD disrupts the association of NEMO with IKKβ,<sup>38</sup> maybe blocking canonical NFκB-signaling pathway activation in osteoblasts and suppressing inflammation (Figure 11). Nevertheless, we need to evaluate the therapeutic potential of NBD peptides by further studying the destructive potential of the immune system.

Current animal models of osteomyelitis are generally achieved by implanting foreign bodies. Although this technology is relatively mature, implanting foreign bodies cannot usually support the healing of infected wounds without removal of the implants. As such, we chose the model described by Nijhof et al,<sup>27</sup> which induce infection by injection of a bacterial suspension, but not implant infections. The osteomyelitis model is associated with significant variation in the intensity of local infection. In our study, there was no significant difference in the intensity of bone infection among the four groups. Laboratory and radiological parameters allowed monitoring of bacterial spread, though were useless for assessing local bone infection. Nevertheless, all animals clearly showed establishment of active infection through local clinical signs at 4 weeks, indicating that the infection was limited to the tibia, confirming the effectiveness of this animal model. In the existing osteomyelitis model, due to the difference in the intensity of infection, the use of morrhuate sodium to evaluate the preventive effect of NBD peptides on chronic bone infection has certain limitations, but this model is suitable for research on the safety of intervention.

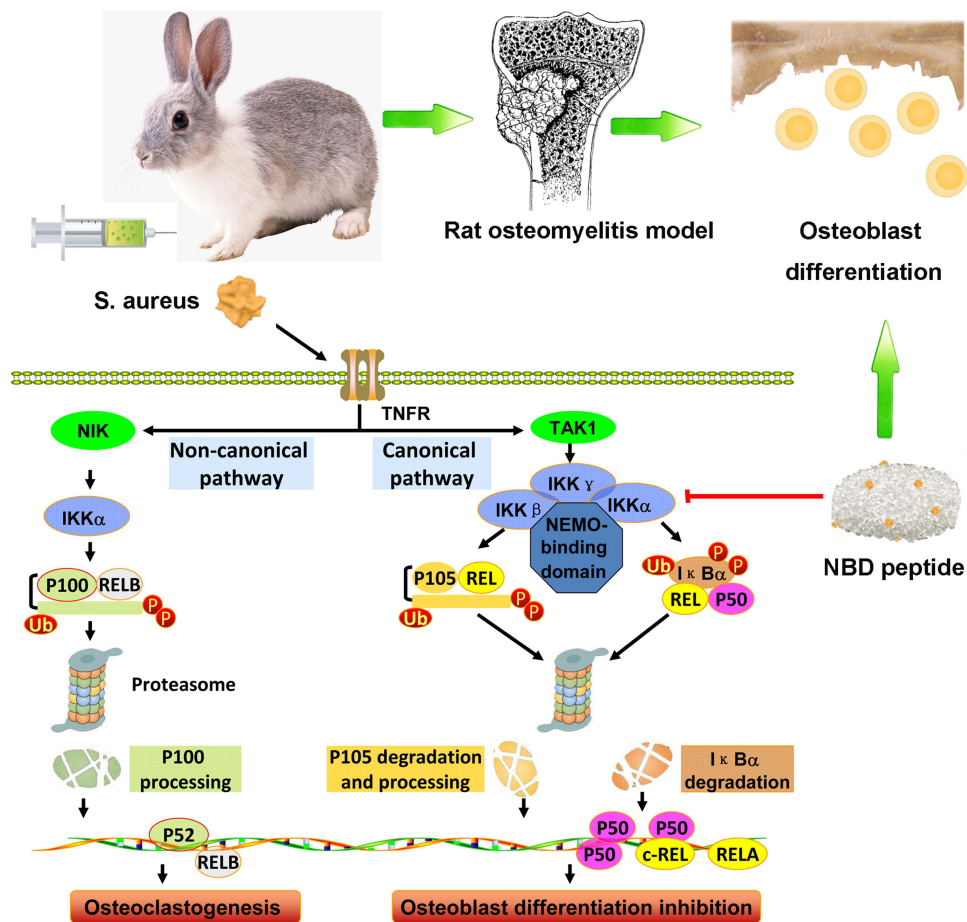


**Figure 11** Diagram of proposed mechanisms by which NBD peptides selectively attenuate inflammation-induced activation of NFκB through interaction with NBD-NEMO and further abrogates (at least partly) the bad influence of inflammation on osteoblast differentiation in an *S. aureus*-induced bone-infection model.  
**Abbreviations:** TNFR, TNF receptor; NBD, NEMO-binding domain; NEMO, NFκB essential modulator.

This study has its limitations, starting with the absence of a sham group with NBD-peptide administration. Therefore, we could not clarify the specific role of NBD peptides in stimulating bone-defect repair. The sample was relatively small, although larger than that of previous experiments. We just explore the effect of single-dose NBD peptides only and thus could not assess potential dose–effect relationship in prophylaxis for bone infection. Last but not least, we were unable to provide extensive long-term safety assessment of NBD peptides to prevent bone infection, especially their destructive potential in the immune system. Due to sex differences in bone formation, we used male rabbits to evaluate new bone–formation effect of NBD peptides to eliminate the effect of sex differences (such as hormone levels) on osteogenesis. Nonetheless, we argue that this study offers a number of important insights into NBD peptides, which were almost equivalent to cefazolin in the context of bone-infection prevention.

## Conclusion

Our in vivo study demonstrated that NBD peptides can be used as prophylaxis for *S. aureus*–associated osteomyelitis, effectively promoting bone-defect repair and indicating the potential of NBD as a preventive option for bone infections in the future.

## Ethics

This study was approved by the animal ethics committee of Nanfang Hospital, Southern Medical University (NFYY-2015-61).

## Acknowledgments

This work was supported by the National Natural Science Foundation of China (81972083), Science and Technology Planning Project of Guangzhou (202102080052, 202102010057, 201804010226), Science Foundation of Guangdong Second Provincial General Hospital (3D-A2020004, 3D-A2020002, YQ2019-009, 2019BSGZ012), Natural Science Foundation of Xinjiang Province (2018D01C014), Minority Science, Technology Talent Special Training Program Project of Xinjiang Province (2019D03025), and The Project of Guangzhou Science and Technology Plan (202102010057). In addition, thanks for the inimitable care and support of Xiao-Jie Zheng over the years. Wen-Jiao Wu and Chang-Liang Xia are co-first authors for this study.

## Disclosure

All authors state that they have nothing to disclose and report no conflicts of interest in this work.

## References

1. Lew DP, Waldvogel FA. Osteomyelitis. *Lancet*. 2004;364(9431):369–379. doi:10.1016/S0140-6736(04)16727-5
2. Pincus DJ, Armstrong MB, Thaller SR. Osteomyelitis of the craniofacial skeleton. *Semin Plast Surg*. 2009;23(2):73–79. doi:10.1055/s-0029-1214159
3. Baur DA, Altay MA, Flores-Hidalgo A, Ort Y, Queresy FA. Chronic osteomyelitis of the mandible: diagnosis and management—an institution’s experience over 7 years. *J Oral Maxillofac Surg*. 2015;73(4):655–665. doi:10.1016/j.joms.2014.10.017
4. Haeffs TH, Scott CA, Campbell TH, Chen Y, August M. Acute and chronic suppurative osteomyelitis of the jaws: a 10-year review and assessment of treatment outcome. *J Oral Maxillofac Surg*. 2018;76(12):2551–2558. doi:10.1016/j.joms.2018.05.040
5. Bury DC, Rogers TS, Dickman MM. Osteomyelitis: diagnosis and treatment. *Am Fam Physician*. 2021;104(4):395–402.
6. Azuma Y, Kaji K, Katogi R, Takeshita S, Kudo A. Tumor necrosis factor-alpha induces differentiation of and bone resorption by osteoclasts. *J Biol Chem*. 2000;275(7):4858–4864. doi:10.1074/jbc.275.7.4858
7. Yamashita M, Otsuka F, Mukai T, et al. Simvastatin antagonizes tumor necrosis factor-alpha inhibition of bone morphogenetic proteins-2-induced osteoblast differentiation by regulating Smad signaling and Ras/Rho-mitogen-activated protein kinase pathway. *J Endocrinol*. 2008;196(3):601–613. doi:10.1677/JOE-07-0532
8. Sacco R, Shah S, Leeson R, et al. Osteonecrosis and osteomyelitis of the jaw associated with tumour necrosis factor-alpha (TNF- $\alpha$ ) inhibitors: a systematic review. *Br J Oral Maxillofac Surg*. 2020;58(1):25–33. doi:10.1016/j.bjoms.2019.09.023
9. Taddio A, Zennaro F, Pastore S, Cimaz R. An update on the pathogenesis and treatment of chronic recurrent multifocal osteomyelitis in children. *Paediatr Drugs*. 2017;19(3):165–172. doi:10.1007/s40272-017-0226-4
10. Suda T, Takahashi N, Udagawa N, Jimi E, Gillespie MT, Martin TJ. Modulation of osteoclast differentiation and function by the new members of the tumor necrosis factor receptor and ligand families. *Endocr Rev*. 1999;20(3):345–357. doi:10.1210/edrv.20.3.0367
11. Deutschmann A, Mache CJ, Bodo K, Zebedin D, Ring E. Successful treatment of chronic recurrent multifocal osteomyelitis with tumor necrosis factor-alpha blockade. *Pediatrics*. 2005;116(5):1231–1233. doi:10.1542/peds.2004-2206

12. Zhang YH, Heulsmann A, Tondravi MM, Mukherjee A, Abu-Amer Y. Tumor necrosis factor-alpha (TNF) stimulates RANKL-induced osteoclastogenesis via coupling of TNF type 1 receptor and RANK signaling pathways. *J Biol Chem.* 2001;276(1):563–568. doi:10.1074/jbc.M008198200
13. Yamamoto Y, Kim DW, Kwak YT, Prajapati S, Verma U, Gaynor RB. IKKgamma/NEMO facilitates the recruitment of the IκappaB proteins into the IκappaB kinase complex. *J Biol Chem.* 2001;276(39):36327–36336. doi:10.1074/jbc.M104090200
14. Claro T, Widaa A, McDonnell C, Foster TJ, O'Brien FJ, Kerrigan SW. Staphylococcus aureus protein A binding to osteoblast tumour necrosis factor receptor 1 results in activation of nuclear factor kappa B and release of interleukin-6 in bone infection. *Microbiology.* 2013;159(Pt 1):147–154. doi:10.1099/mic.0.063016-0
15. Sun SC. The non-canonical NF-κB pathway in immunity and inflammation. *Nat Rev Immunol.* 2017;17(9):545–558. doi:10.1038/nri.2017.52
16. Strickland I, Ghosh S. Use of cell permeable NBD peptides for suppression of inflammation. *Ann Rheum Dis.* 2006;65 Suppl 3(Suppl3):iii75–iii82. doi:10.1136/ard.2006.058438
17. Zhao J, Zhang L, Mu X, et al. Development of novel NEMO-binding domain mimetics for inhibiting IKK/NF-κB activation. *PLoS Biol.* 2018;16(6):e2004663. doi:10.1371/journal.pbio.2004663
18. Luo Q, Li D, Bao B, et al. NEMO-binding domain peptides alleviate perihematomal inflammation injury after experimental intracerebral hemorrhage. *Neuroscience.* 2019;409:43–57. doi:10.1016/j.neuroscience.2019.04.041
19. Sun Y, Li X, Zhang L, et al. Cell permeable NBD peptide-modified liposomes by hyaluronic acid coating for the synergistic targeted therapy of metastatic inflammatory breast cancer. *Mol Pharm.* 2019;16(3):1140–1155. doi:10.1021/acs.molpharmaceut.8b01123
20. Tas SW, Vervoordeldonk MJ, Hajji N, May MJ, Ghosh S, Tak PP. Local treatment with the selective IκappaB kinase beta inhibitor NEMO-binding domain peptide ameliorates synovial inflammation. *Arthritis Res Ther.* 2006;8(4):R86. doi:10.1186/ar1958
21. Clohisy JC, Yamanaka Y, Faccio R, Abu-Amer Y. Inhibition of IKK activation, through sequestering NEMO, blocks PMMA-induced osteoclastogenesis and calvarial inflammatory osteolysis. *J Orthop Res.* 2006;24(7):1358–1365. doi:10.1002/jor.20184
22. Dai S, Hirayama T, Abbas S, Abu-Amer Y. The IκappaB kinase (IKK) inhibitor, NEMO-binding domain peptide, blocks osteoclastogenesis and bone erosion in inflammatory arthritis. *J Biol Chem.* 2004;279(36):37219–37222. doi:10.1074/jbc.C400258200
23. Liu YD, Yang HX, Liao LF, et al. Systemic administration of strontium or NBD peptide ameliorates early stage cartilage degradation of mouse mandibular condyles. *Osteoarthritis Cartil.* 2016;24(1):178–187. doi:10.1016/j.joca.2015.07.022
24. Reay DP, Yang M, Watchko JF, et al. Systemic delivery of NEMO binding domain/IKKγ inhibitory peptide to young mdx mice improves dystrophic skeletal muscle histopathology. *Neurobiol Dis.* 2011;43(3):598–608. doi:10.1016/j.nbd.2011.05.008
25. Jimi E, Aoki K, Saito H, et al. Selective inhibition of NF-κappa B blocks osteoclastogenesis and prevents inflammatory bone destruction in vivo. *Nat Med.* 2004;10(6):617–624. doi:10.1038/nm1054
26. Li W, Yu B, Li M, et al. NEMO-binding domain peptide promotes osteoblast differentiation impaired by tumor necrosis factor alpha. *Biochem Biophys Res Commun.* 2010;391(2):1228–1233. doi:10.1016/j.bbrc.2009.12.048
27. Nijhof MW, Stallmann HP, Vogely HC, et al. Prevention of infection with tobramycin-containing bone cement or systemic cefazolin in an animal model. *J Biomed Mater Res.* 2000;52(4):709–715. doi:10.1002/1097-4636(20001215)52:4<709::AID-JBM16>3.0.CO;2-W
28. Norden CW, Myerowitz RL, Keleti E. Experimental osteomyelitis due to Staphylococcus aureus or Pseudomonas aeruginosa: a radiographic-pathological correlative analysis. *Br J Exp Pathol.* 1980;61(4):451–460.
29. Smeltzer MS, Thomas JR, Hickmon SG, et al. Characterization of a rabbit model of staphylococcal osteomyelitis. *J Orthop Res.* 1997;15(3):414–421. doi:10.1002/jor.1100150314
30. Komori T. Runx2, an inducer of osteoblast and chondrocyte differentiation. *Histochem Cell Biol.* 2018;149(4):313–323. doi:10.1007/s00418-018-1640-6
31. An J, Yang H, Zhang Q, et al. Natural products for treatment of osteoporosis: the effects and mechanisms on promoting osteoblast-mediated bone formation. *Life Sci.* 2016;147:46–58. doi:10.1016/j.lfs.2016.01.024
32. Oviedo-Boyso J, Cortés-Vieyra R, Huante-Mendoza A, et al. The phosphoinositide-3-kinase-Akt signaling pathway is important for Staphylococcus aureus internalization by endothelial cells. *Infect Immun.* 2011;79(11):4569–4577. doi:10.1128/IAI.05303-11
33. Zhu F, Yue W, Wang Y. The nuclear factor kappa B (NF-κB) activation is required for phagocytosis of staphylococcus aureus by RAW 264.7 cells. *Exp Cell Res.* 2014;327(2):256–263. doi:10.1016/j.yexcr.2014.04.018
34. Lan Y, Xie H, Shi Y, et al. NEMO-binding domain peptide ameliorates inflammatory bone destruction in a Staphylococcus aureus-induced chronic osteomyelitis model. *Mol Med Rep.* 2019;19(4):3291–3297. doi:10.3892/mmr.2019.9975
35. Xu CP, Chen Y, Sun HT, et al. Efficacy of NEMO-binding domain peptide used to treat experimental osteomyelitis caused by methicillin-resistant Staphylococcus aureus: an in-vivo study. *Antimicrob Resist Infect Control.* 2019;8:182. doi:10.1186/s13756-019-0627-y
36. Prokusi L. Prophylactic antibiotics in orthopaedic surgery. *J Am Acad Orthop Surg.* 2008;16(5):283–293. doi:10.5435/00124635-200805000-00007
37. Gollwitzer H, Roessner M, Langer R, et al. Safety and effectiveness of extracorporeal shockwave therapy: results of a rabbit model of chronic osteomyelitis. *Ultrasound Med Biol.* 2009;35(4):595–602. doi:10.1016/j.ultrasmedbio.2008.10.004
38. May MJ, D'Acquisto F, Madge LA, Glöckner J, Pober JS, Ghosh S. Selective inhibition of NF-κappaB activation by a peptide that blocks the interaction of NEMO with the IκappaB kinase complex. *Science.* 2000;289(5484):1550–1554. doi:10.1126/science.289.5484.1550